JOINT TRANSPORTATION
RESEARCH PROGRAM
INDIANA DEPARTMENT OF TRANSPORTATION
AND PURDUE UNIVERSITY

Field Implementation of Concrete Strength Sensor to Determine Optimal Traffic Opening Time

Zhihao Kong, Na Lu

SPR-4753 • Report Number: FHWA/IN/JTRP-2024/05 • DOI: 10.5703/1288284317724

RECOMMENDED CITATION

Kong, Z., & Lu, N. (2024). *Field implementation of concrete strength sensor to determine optimal traffic opening time* (Joint Transportation Research Program Publication No. FHWA/IN/JTRP-2024/05). West Lafayette, IN: Purdue University. https://doi.org/10.5703/1288284317724

AUTHORS

Zhihao Kong
Graduate Research Assistant
Lyles School of Civil Engineering
Purdue University

Na Lu, PhD
Associate Dean of Faculty of College of Engineering
Reilly Professor
Lyles School of Civil Engineering
Purdue University
(765) 494-5842
luna@purdue.edu
Corresponding Author

JOINT TRANSPORTATION RESEARCH PROGRAM

The Joint Transportation Research Program serves as a vehicle for INDOT collaboration with higher education institutions and industry in Indiana to facilitate innovation that results in continuous improvement in the planning, design, construction, operation, management and economic efficiency of the Indiana transportation infrastructure. https://engineering.purdue.edu/JTRP/index_html

Published reports of the Joint Transportation Research Program are available at http://docs.lib.purdue.edu/jtrp/.

NOTICE

TECHNICAL REPORT DOCUMENTATION PAGE

1. Report No. FHWA/IN/JTRP-2024/07	**2. Government Accession No.**	**3. Recipient's Catalog No.**
4. Title and Subtitle Field Implementation of Concrete Strength Sensor to Determine Optimal Traffic Opening Time		**5. Report Date** December 2023 **6. Performing Organization Code**
7. Author(s) Zhihao Kong and Na (Luna) Lu		**8. Performing Organization Report No.** FHWA/IN/JTRP-2024/07
9. Performing Organization Name and Address Joint Transportation Research Program Hall for Discovery and Learning Research (DLR), Suite 204 207 S. Martin Jischke Drive West Lafayette, IN 47907		**10. Work Unit No.** **11. Contract or Grant No.** SPR-4753
12. Sponsoring Agency Name and Address Indiana Department of Transportation (SPR) State Office Building 100 North Senate Avenue Indianapolis, IN 46204		**13. Type of Report and Period Covered** Final Report **14. Sponsoring Agency Code**

15. Supplementary Notes

Conducted in cooperation with the U.S. Department of Transportation, Federal Highway Administration.

16. Abstract

In the fast-paced and time-sensitive fields of construction and concrete production, real-time monitoring of concrete strength is crucial. Traditional testing methods, such as hydraulic compression (ASTM C 39) and maturity methods (ASTM C 1074), are often laborious and challenging to implement on-site. Building on prior research (SPR-4210 and SPR-4513), we have advanced the electromechanical impedance (EMI) technique for in-situ concrete strength monitoring, which is crucial for determining safe traffic opening times. These projects have made significant strides in technology, including the development of an IoT-based hardware system for wireless data collection and a cloud-based platform for efficient data processing. A key innovation is the integration of machine learning tools, which not only enhance immediate strength predictions but also facilitate long-term projections vital for maintenance and asset management.

To bring this technology to practical use, we collaborated with third-party manufacturers to set up a production line for the sensor and datalogger assembly. The system was extensively tested in various field scenarios, including pavements, patches, and bridge decks. Our refined signal processing algorithms—benchmarked against a mean absolute percentage error (MAPE) of 16%, which is comparable to the ASTM C39 interlaboratory variance of 14%—demonstrate reliable accuracy. Additionally, we have developed a comprehensive user manual to aid field engineers in deploying, connecting, and maintaining the sensing system, paving the way for broader implementation in real-world construction settings.

17. Key Words concrete, sensor, piezoelectric, electromechanical impedance, EMI, open traffic, strength, sensing, nondestructive evaluation, NDT, wireless, database, internet of things	**18. Distribution Statement** No restrictions. This document is available through the National Technical Information Service, Springfield, VA 22161.

19. Security Classif. (of this report) Unclassified	**20. Security Classif. (of this page)** Unclassified	**21. No. of Pages** 31	**22. Price**

Form DOT F 1700.7 (8-72) Reproduction of completed page authorized

EXECUTIVE SUMMARY

Introduction

In the fast-paced and time-sensitive fields of construction and concrete production, real-time monitoring of concrete strength is crucial. Traditional testing methods, such as hydraulic compression (ASTM C 39) and maturity methods (ASTM C 1074, 2017), are often laborious and challenging to implement on-site. Building on the prior research of SPR-4210 (Su et al., 2020) and SPR-4513 (Kong & Lu, 2023), INDOT has advanced the electromechanical impedance (EMI) technique for in-situ concrete strength monitoring, which is crucial for determining safe traffic opening times. This project has made significant strides in technology, including the development of an IoT-based hardware system for wireless data collection and a cloud-based platform for efficient data processing. A key innovation is the integration of machine learning tools, which not only enhance immediate strength predictions but also facilitate long-term projections vital for maintenance and asset management.

To bring this technology into practical use, we collaborated with third-party manufacturers to set up a production line for the sensor and datalogger assembly. The system was extensively tested in various field scenarios, including pavements, patches, and bridge decks. Our refined machine learning algorithms, benchmarked against a mean absolute percentage error (MAPE) of 16%, which is comparable to the ASTM C39 interlaboratory variance of 14% for three cylinders, demonstrate reliable accuracy. Additionally, we have developed a comprehensive user manual to aid field engineers in deploying, connecting, and maintaining the sensing system, which paves the way for broader implementation in real-world construction settings.

Findings

In this innovative project, our research team collaborated with a renowned Chicago-based manufacturer, leveraging their extensive, several-decade expertise in Printed Circuit Board (PCB) production, mechanical design, and molding. We identified and established key manufacturing parameters and processes that are critical for the efficient and high-quality production of our sensors and data loggers. Embracing industrial techniques such as injection molding, Surface Mount Technology (SMT), and metered mixing, we have successfully scaled up to mass production.

Our research extended to the Department of Transportation in various states, leading to the successful deployment of our products. A significant achievement of this project was the development of a comprehensive machine learning platform that facilitates real-time prediction of concrete strengths and future strength projections. This end-to-end training and inferencing platform is a testament to our commitment to advance concrete monitoring technology.

Moreover, we created a detailed user guide tailored for users with limited knowledge of sensing technology. This guide simplifies the installation process and data interpretation, making our technology accessible to a broader audience. The major findings and outcomes of this project, which mark a significant step forward in the field of concrete strength monitoring, are presented in the following sections.

1. *Production line optimization for sensing system hardware.*

   The research has led to significant advancements in the development of the sensing system's hardware production line. We identified and optimized critical parameters and procedures. Key among these was the refinement of geometric factors, such as the thickness of the acoustic sensor's sealing layer and the diameter of the piezoelectric component. These optimizations were carefully balanced to ensure both high sensor performance and manufacturability. In our pursuit of excellence, we sourced piezoelectric components from specialized suppliers, specifying material parameters like the frequency constant to meet our stringent requirements. This approach ensured consistent quality and performance of these critical components. Additionally, the components of the data logger were meticulously selected based on their availability and suitability for our needs. Recognizing the demanding environments in which these systems operate, the data logger underwent a comprehensive redesign to enhance its durability and resilience against harsh conditions. This redesign underscored our commitment to creating robust and reliable hardware for our sensing systems.

2. *Advancements in cloud platforms for data storage and computation.*

   Building on the momentum from our previous project (SPR-4513), we significantly upgraded our cloud computation and storage platform. This revamped platform integrated a database, data telemetry, an IoT hub, and machine learning pipelines within a unified Microsoft Azure workspace. The integration of these components offers numerous advantages, including enhanced server resource management, improved safety protocols, streamlined automated machine learning processes for training and inferencing, and the ability to swiftly deploy and roll back codes. To maximize efficiency and minimize interference, we divided the cloud platform into three distinct stages: production, development, and research. Each stage operates with its independent databases and environments, ensuring that activities in one stage do not disrupt or conflict with those in another. A notable innovation in our approach is the adoption of transfer learning techniques. This strategy effectively bridges the gap between field and laboratory data, resulting in a marked improvement in the performance of our machine learning models. This enhancement is crucial for the accurate and reliable application of our technology in real-world settings.

3. *Creation of an accessible user guide for a general audience.*

   Recognizing the importance of making our technology accessible to all, we meticulously developed a comprehensive user guide for our sensing system. This guide was specifically designed to be user-friendly for individuals who may not have prior knowledge or experience with sensors or dataloggers. It is a key resource, enabling users from a wide range of backgrounds to confidently utilize our products.

   The user guide covers several critical aspects and provides step-by-step instructions for the installation of the sensor, ensuring users can set it up efficiently and correctly. Maintenance procedures for the datalogger are clearly outlined, helping users preserve the longevity and effectiveness of the device. Guidance on navigating and utilizing the

dashboard of our cloud system is included, allowing users to effortlessly manage and monitor their data. Additionally, the guide includes detailed instructions for data retrieval, ensuring that users can easily access and interpret the data collected by the system. This guide makes our advanced technology approachable and usable for everyone, irrespective of their technical background.

Implementation

In the implementation phase of the project, we collaborated with eight State Departments of Transportation (DOTs) to deploy and rigorously test our sensing system. This comprehensive field testing focused on evaluating both the reliability and accuracy of the system under real-world conditions. To achieve this, we established a specialized civil engineering task force that traveled across the country. The mission was to create our own beam and cylinder samples and to ensure these samples were cured under controlled conditions, including air curing on-site and water bath curing in laboratory settings. This approach allowed us to test our system under a variety of realistic scenarios. Remarkably, our dataloggers and sensors withstood most harsh field conditions, demonstrating resilience against high temperatures, elevated humidity levels, and rain. These findings were important, as they confirmed the robustness of our sensing hardware in challenging construction environments. Furthermore, the results from these field tests validated the accuracy of our inference model, underscoring its potential for widespread application in the construction industry.

CONTENTS

LIST OF TABLES

LIST OF FIGURES

1. INTRODUCTION

1.1 Research Background

Concrete structures are often exposed to substantial loading even at their early age, which may cause premature failure or significant reduction in their life span. Therefore, it is critical to develop an in-situ NDT method that can determine the mechanical properties of concrete in real-time. In particular, strength (the maximum stress value in the stress-strain) stands as one of most important mechanical properties in concrete structures.

The electromechanical impedance (EMI) method has been established as an effective on-site technique for assessing the properties of cementitious materials, such as compressive strength and Young's modulus. This method offers an alternative to traditional hydraulic compression tests. Fundamentally, the EMI technique employs piezoelectric materials like lead zirconate titanate (PZT) as transducers to gauge the mechanical characteristics of host structures. This is due to PZT's capability to directly transform mechanical vibrations into alternating current (AC) and vice versa. When PZT sensors vibrate in response to interactions with the host structure, they produce electrical signals in the form of admittance and impedance. These signals are indicative of the mechanical properties of the structure being analyzed.

The EMI method offers the advantage of measuring dynamic modulus using just a single sensor, making it a convenient option for on-site testing of concrete structures. The process is straightforward, involving either attaching the sensor to the surface of the specimen or embedding it within, and then linking it to an impedance analyzer. This is in contrast to other stress wave-based methods like Ultrasonic Pulse Velocity (UPV) and Impact Resonance (IR), which necessitate a setup with at least a transmitter and receiver. Consequently, the EMI technique results in considerable savings in terms of time, labor, and costs.

We demonstrated the feasibility of measuring the in-place strength of concrete structures using our patent pending REBEL Concrete Strength Monitoring System (Figure 1.1 and Figure 1.2), during our effort in SPR-4210 and SPR-4513. We have approved that our invention is at the cutting edge of concrete sensor solutions and is pioneering technologies that would replace century-old destructive testing methods. The success of this technology will not only disrupt concrete industry, but also have broader impacts on increasing the economic competitiveness of the United States and advancing the welfare of the American public. Our technology is established on sophisticated science and engineering principles. Specifically, it leverages the physics of mechanical wave vibration, wireless data collection/communication, Artificial Intelligence (AI) powered signal processing algorithms and cloud computing systems. By using this technology, users can avoid the hassle of preparing concrete cylinder samples, inconsistent testing results caused by compression testing, and the limited number of tests that hinder real-time, data-driven decisions during construction. The previous SPR projects enabled our research team to establish a highly functional development team, conduct the field-test of a prototype product, and perform in-depth customer and market studies nationwide. The novelty and impact of the technology are recognized by numerous awards including the 2021 ASCE Game Changer, the 2022 ASCE Alfred Noble Prize by American Society of Civil Engineering, and 2022's Next Big Things in Tech in Transportation Sector by Fast Company. Notably, our sensing method has been approved by the AASHTO technical committee and will be published as a formal testing standard.

1.2 Objectives

The primary aim of this implementation project is to establish standardized testing procedures and protocols for the field application of the concrete strength sensor, a collaborative development by Purdue University and INDOT. This initiative focuses on monitoring key properties of concrete structures, particularly the set time and strength development profile. An integral part

Figure 1.1 Dashboard of REBEL concrete strength monitoring system.

Figure 1.2 Hardware of REBEL concrete strength monitoring system.

of this project is a thorough cost-benefit analysis of the method, coupled with developing recommendations for optimal traffic opening times and maintenance schedules. The project's objectives are strategically outlined as follows.

1. Establish a production line for assembling the hardware system required for testing, ensuring efficiency and scalability in manufacturing.
2. Deploy the concrete strength sensing system in a variety of Indiana's pavement and bridge projects, demonstrating its applicability in real-world infrastructural contexts.
3. Develop standard testing protocols and provide training to state engineers, empowering them to effectively utilize these advanced sensing methods.
4. Create a centralized, cloud-based computational platform designed to process sensor data. This platform will utilize sophisticated machine learning models to analyze and interpret the data accurately.
5. Develop user-friendly applications and devise strategic implementation plans. These plans will guide how different stakeholders can leverage the concrete sensing technology in various use cases, ensuring broad and effective application of this innovative technology.

1.3 Organization of the Report

This report consists of five chapters. This first chapter introduces the background and objective of this research. The second chapter reviews existing concrete strength estimation methods. The third chapter reports our progress in the sensing system, including both hardware and software. The fourth chapter presents the field implementation of the improved sensing system. The final chapter summarizes the current works and concludes this report.

2. LITERATURE REVIEW

2.1 Traditional Testing Methods for Strength of Concrete

The compressive strength test is a commonly employed method to assess the strength of concrete. It involves applying a compressive force to a concrete sample until it fractures, and then recording the peak load sustained by the specimen (as shown in Figure 2.1). While this technique is straightforward and widely recognized in the industry as the benchmark for determining concrete strength, it can be prone to errors. These inaccuracies often arise from challenges in ensuring uniform loading and the influence of the specimen's size and shape. Research (del Viso et al., 2008) has indicated that concrete samples with greater slenderness ratios often exhibit reduced strength.

Another approach to evaluate concrete compressive strength is the core test. This involves extracting a concrete core from the structure (illustrated in Figure 2.2) and measuring its maximum compressive strength under a load. The core test offers a more precise reflection of the concrete's in-situ strength. However, this method can be more labor-intensive and expensive compared to standard compressive strength testing.

The rebound hammer test, also known as the "Schmidt Hammer" test, is a non-destructive evaluation (NDE) technique utilized to approximate the compressive strength of concrete. This method involves using a rebound hammer to gauge the rebound distance of a steel ball after it impacts the concrete surface (as shown in Figure 2.3). The measured rebound distance is

Figure 2.1 A typical compression testing setup.

subsequently correlated to a specific compressive strength value. While the rebound hammer test is a rapid and straightforward method, its accuracy can be compromised by surface irregularities, and it does not offer a precise measurement of the in-situ strength of concrete (Shariati et al., 2011).

The maturity test is a widely used technique for assessing early-age concrete hydration by monitoring its temperature change. This method is based on the understanding that the strength development in concrete is linked to the heat generated from the chemical reaction between cementitious materials (like cement and supplementary materials) and water. It involves using the recorded temperature history to estimate the concrete's strength gain. The standard ASTM C1074 (ASTM, 2017) outlines a procedure (illustrated in Figure 2.4) for evaluating concrete strength using the maturity method. However, this test depends on strength-maturity curves established in the laboratory, which can vary considerably from in-situ field results, mainly due to ambient temperature effects. Additionally, it requires recalibration for each new concrete mix, making it less practical for field use.

In summary, core drilling offers higher accuracy but is less efficient; the rebound hammer is more user-friendly but less precise. The maturity method's need for recalibration with each concrete mix makes it inconvenient. Despite various influencing factors like specimen geometry, fabrication process, and loading speed, the hydraulic compression test remains the most accepted method for concrete strength testing due to its simplicity and cost-effectiveness.

Figure 2.2 A typical core drilling setup (Shin et al., 2008).

2.2 NDE Methods for Mechanical Properties of Concrete

2.2.1 Choosing Metrics and Categorizing Methods

To evaluate the mechanical properties of concrete, a range of physical metrics has been considered. Acoustic or ultrasonic methods involve using mechanical waves to determine the dynamic modulus of concrete in situ. This group includes techniques such as Impact Echo (IE), Impact Resonance (IR), Ultrasonic Pulse Velocity (UPV), Electro-mechanical Impedance Spectroscopy (EMI), and Surface Acoustic Wave (SAW). The interaction of mechanical waves

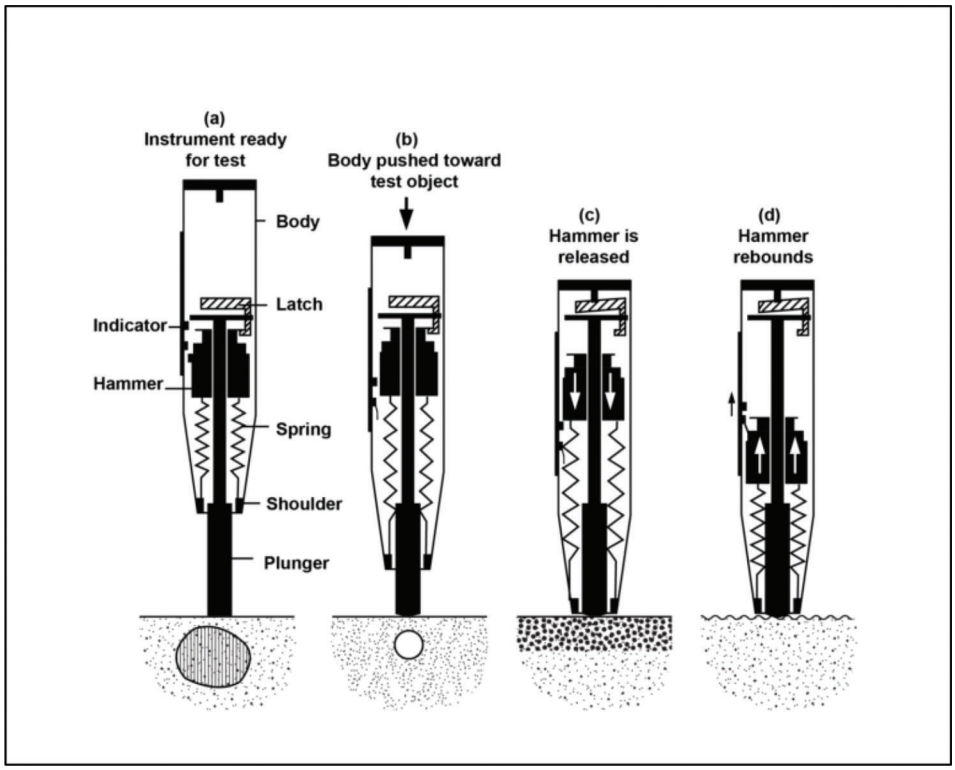

Figure 2.3 Rebound hammer (Smith, 2005).

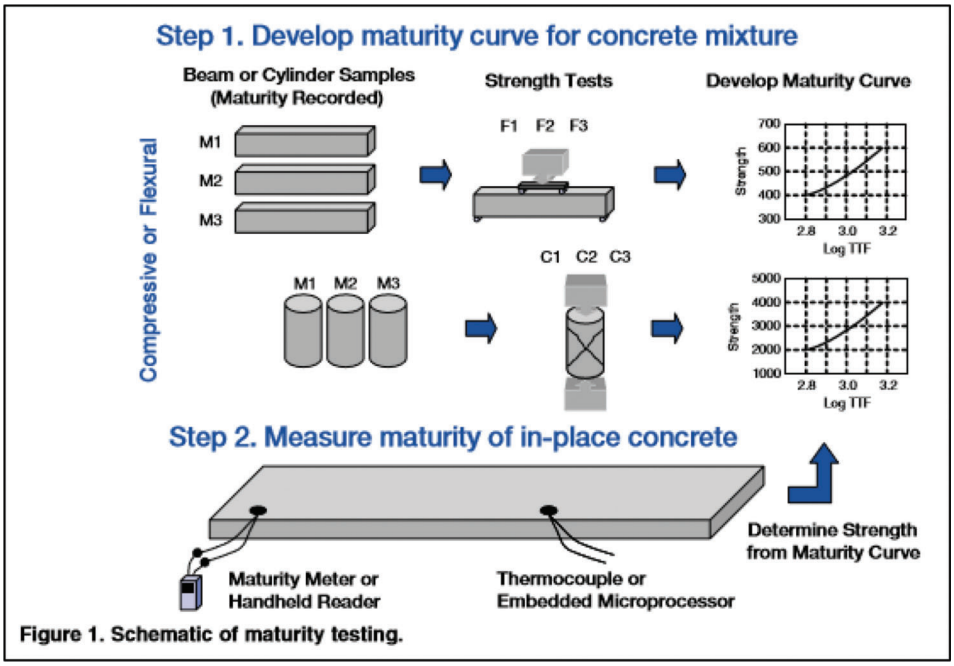

Figure 2.4 Maturity testing (Smith, 2005).

with a material, which causes disturbances like particle displacement, is influenced by the material's mechanical characteristics (density, dynamic modulus, viscosity, etc.). Thus, acoustic, or ultrasonic methods are inherently aligned with the objectives of this study.

Optical or electromagnetic methods employ light or electromagnetic waves as the probing signal. This category encompasses optical fiber and Ground Penetrating Radar (GPR). The hydration process in concrete, which leads to an increase in elastic modulus and strength, also affects the water content, influencing how electromagnetic waves propagate through the material. Consequently, these methods are more suited to monitoring relative changes in concrete properties rather than providing absolute measurements.

The thermal category includes the maturity method, designated for strength monitoring in ASTM C1074. It utilizes accumulated heat from hydration as the measurement metric, correlating it with concrete strength development. However, extensive calibration, specific to each concrete mix, is required to establish this relationship, making the method valuable but inefficient.

The electrical category comprises the electrical resistivity method. Similar to the electromagnetic approach, it tracks changes in water content during hydration but does not directly measure the concrete's mechanical properties. In summary, acoustic metrics are the most closely related to the desired target values in terms of physical similarity. The following sections will delve into the application of various acoustic methods in monitoring the mechanical properties of concrete.

2.2.2 Impact Echo Method

Impact Echo (IE) is a longstanding non-destructive testing technique widely used in engineering (ASTM, 2022; Carino, 2001, 2015; Gibson & Popovics, 2005; Popovics, 1997; Villain et al., 2009). Developed in 1986 by the National Institute of Standards and Technology (NIST) and Cornell University, the IE method was specifically designed for assessing concrete structures. This technique operates on the principle of low-frequency elastic waves, analyzing the transient response of a structure following a mechanical impact.

The IE method has demonstrated its versatility and applicability in various situations, particularly in measuring the thickness of slabs and cylinder walls. Additionally, it has been effectively employed to identify flaws in a range of materials, including concrete and masonry. Theoretical studies on the IE method have shed light on its underlying mechanisms. It was found that the impact echo resonance in a plate's thickness direction correlates with the zero-group-velocity (ZGV) frequency of the S_1 Lamb wave mode, as illustrated in Figure 2.5. This discovery provided a theoretical basis for a correction factor that was previously used empirically, enhancing the method's accuracy and reliability in practical applications.

2.2.3 Ultrasonic Pulse Velocity

Ultrasonic Pulse Velocity (UPV) relies on transmitting ultrasonic waves through a material and measuring their time of flight (TOF). This TOF measurement is then used to determine the wave velocity, which in

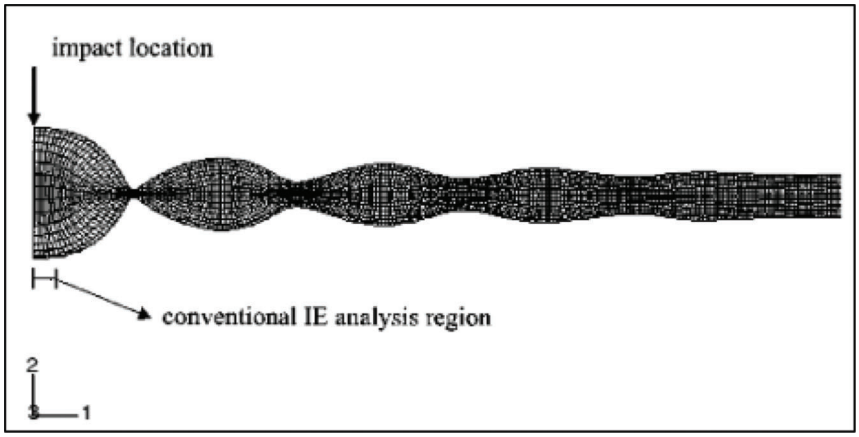

Figure 2.5 Vibration mode shape of IE resonance of a slab (Gibson & Popovics, 2005).

turn gives insights into the material's elasticity. The testing setup of UPV is shown in Figure 2.6. A key characteristic of UPV is its ability to detect flaws—slower wave velocities often indicate the presence of pores, cracks, or overall poor quality in concrete. While UPV is specified in ASTM C597 (ASTM, 2016), the standard explicitly states that it should not be used as a definitive measure of strength, nor should it be the sole test for confirming the modulus of elasticity of field concrete as assumed in design. Instead, the longitudinal resonance method in Test Method C215 is recommended for determining the dynamic modulus of elasticity.

Despite this, there have been numerous applications of UPV in assessing concrete strength and dynamic modulus, as reported in the literature (Casciaro et al., 2016; Irrigaray et al., 2016; Ju et al., 2017; Latif Al-Mufti & Fried, 2012; Punurai, Jacobs, et al., 2006; Punurai, Jarzynski, et al., 2006; Ye et al., 2003). It is important to note that the formulas converting UPV readings to concrete strength vary based on the material's composition. Thus, UPV shares a limitation with methods like Impact Echo (IE) and Impact Resonance (IR), specifically in translating dynamic mechanical properties to static properties.

Another challenge with the UPV method is its requirement for a pair of ultrasound transducers, which can be costly. This expense limits its application primarily to surface-mounted setups or through-transmission testing on smaller specimens.

2.2.4 Electro-Mechanical Impedance Spectroscopy (EMI)

The Electromechanical Impedance (EMI) method is categorized under stress-wave based sensing methods, yet it stands out from others due to its unique advantages and certain limitations (Ghafari et al., 2018; Han et al., 2020; Kong & Lu, 2020; Su et al., 2019, 2021; Su, Han, Kong et al., 2020; Su, Han, Nantung et al., 2020). One of the primary benefits of the EMI approach for monitoring concrete strength is its simplicity—it requires only a single piezoelectric sensor and combines the transmission-receiving process. This results in an

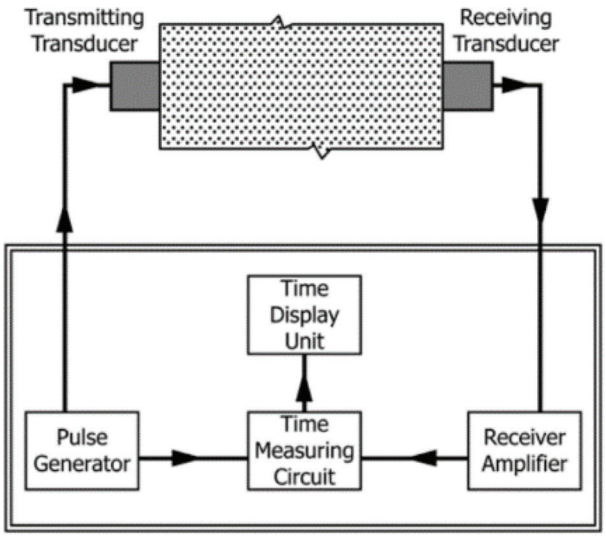

Figure 2.6 UPV testing setup (ASTM C597).

easier setup and reduced hardware costs compared to traditional stress-wave methods. For instance, methods like Ultrasonic Pulse Velocity (UPV) typically need either a pair of transducers serving as separate transmitter and receiver, or a single transducer where the transmission and receiving processes are distinct and separated in time, often requiring an electrical relay or "T-R switch" to alternate the transducer's operational mode.

In various studies, mathematical and numerical models have been developed to understand the interaction between host structures and piezoelectric sensors. These studies, referenced in literature (Bogas et al., 2013; Liang et al., 1994; Narayanan et al., 2017; Wang et al., 2014), simplify the impact of the host structure on the piezoelectric sensor by treating it as a mechanical boundary condition. Additionally, research documented in Fan et al. (2018), Yang and Divsholi (2010) has examined the sensing range of EMI sensors, particularly in detecting impact and saw cut damages. These investigations have found that the effective sensing distance of EMI sensors can span from several tens of centimeters up to approximately half a meter.

Understanding the physical principles behind the Electromechanical Impedance (EMI) sensing technique is crucial, but signal processing is equally important. Signal processing in EMI can be divided into two main categories: spectrum amplitude (Narayanan et al., 2017, 2020) and resonant frequency (Lu et al., 2018). These two metrics are based on different physical principles, which in turn affect the sensor packaging method.

For instance, EMI methods that use spectrum amplitude as a metric are more sensitive to damping effects caused by the sensor packaging materials. Therefore, these methods demand minimal packaging around the piezoelectric element. A study cited in literature (Saravanan et al., 2015) explored a packaging technique using a cement block (smart aggregate) and discovered that the signal was not particularly sensitive to the strength development in the early stages of concrete curing. Typically, the piezoelectric element is covered with a conformal material like a thin epoxy layer in most applications.

On the other hand, EMI methods that utilize spectrum resonant frequency as the metric are more concerned with the sensor's structure and its vibrational mode. This allows for greater flexibility in the design of sensor packaging, as the focus shifts to maintaining the integrity of the sensor's vibration characteristics rather than minimizing damping effects.

3. PRODUCTION LINE OPTIMIZATION FOR SENSING SYSTEM HARDWARE

This chapter reports the work of optimization of hardware of the sensing system for better manufacturability and durability.

3.1 Optimize the Hardware Design and Cost of the REBEL Sensing System

In this phase of the project, we undertook a comprehensive redesign of the REBEL Datalogger, incorporating feedback and insights gained from field trials. The redesign addressed three key areas. First, we identified the necessity of a more advanced and readily available impedance analyzer chip. This standardization is particularly crucial given the REBEL system's reliance on machine learning algorithms for signal processing. Ensuring consistency in impedance measurement hardware is essential to avoid discrepancies in the output of our product's models. Then, the project involved incorporating new features and enhanced functionalities, requiring a redesign of the internal hardware. Notable additions include GPS tracking, sensor-embedded memory, and extended data retention capabilities. These enhancements, while increasing the cost of the device, significantly boost its value to end-users. The GPS tracking feature simplifies sensor location recording and aids in locating lost dataloggers. The support for embedded memory in the sensor allows seamless data attribution to the correct sensor, regardless of the connected datalogger. An expanded internal memory provides a buffer against local cellular outages, ensuring continuous real-time strength predictions. Next, our experience in previous studies highlighted the need for a more robust enclosure for the datalogger, capable of withstanding harsh construction environments. Incidents such as exposure to mortar splashes, immersion in puddles, or drops from considerable heights were observed during previous field trials, leading to physical failures. The new design is secure, cost-efficient, and built to endure such challenging conditions. Unlike the prototype used in our initial study, the new enclosure has a rugged, industrial look and feel. It also includes features like loops for wire-ties and other attachment methods, facilitating easier installation. Figure 3.1, Figure 3.2, and Figure 3.3 illustrate the prototypes of these new datalogger enclosures developed during the project.

3.2 Improved Deployment and User Experience

During this project, we focused on optimizing the installation configuration of the datalogger and sensor to enhance the ease of deployment and user experience, particularly in challenging construction sites like transportation infrastructures (pavements and bridges).

Figure 3.1 Photo of the REBEL datalogger.

Figure 3.2 Photo of the REBEL sensor.

Figure 3.3 Rendered image of the new version of REBEL hardware.

Our team identified the lack of suitable positions for datalogger installation at many construction sites. Our temporary solutions previously used in the field were not only inefficient but also required extra installation effort. To resolve this, we designed and developed a range of installation fixtures tailored to various field conditions. Collaborating closely with our contractor partners, we identified the most common field scenarios and created specialized fixtures, such as ground-fixed posts with small footprints and panels designed for zip tie attachments. These custom-designed fixtures, now part of our production line, are provided as convenient auxiliary tools, streamlining the installation process.

A significant enhancement was made to the datalogger-sensor connection process. Originally, each device had a unique ID that needed manual entry into the REBEL Dashboard by the end user. To simplify this and reduce potential deployment errors, we introduced a system where the sensor now includes embedded memory, readable through the connection cable. This new method requires the user to scan only the QR code on the sensor cable to link it to the REBEL Dashboard. This change not only streamlines the setup process but also enables the storage of calibration and application-specific information on the sensor itself, increasing the system's adaptability for future applications. Our internal team can now access both datalogger and sensor-specific data, alongside live concrete strength, and temperature readings, facilitating more effective diagnostics and problem-solving in the field.

3.3 Optimizing IoT Cloud Infrastructure

We focused on optimizing the IoT cloud infrastructure, addressing challenges and limitations encountered during previous studies. We marked a significant evolution in our approach to managing and expanding the capabilities of our cloud system.

Initially, our cloud system was based on an AWS EC2 instance, which combined various functions like the database, web portal, machine learning inference endpoint, and data telemetry program on a single server. However, with the customer base growing significantly since the initial field trials, it became apparent that this setup would not suffice for large-scale operations. To overcome these limitations, we transitioned to the Microsoft Azure platform, known for its modular design principles and robust capabilities. Azure's architecture allowed us to conceptualize and deploy each cloud component as an independent service. This shift to a decentralized approach, featuring dynamic data pipelines and separate services for IoT Hub and database management, significantly enhanced system resilience and integration of microservices.

A key improvement was the introduction of extensible IoT data pipelines. The previous AWS-based system posed challenges in scalability and feature addition due to its centralized architecture. With Azure, we could easily integrate new microservices into the system. For instance, a novel microservice was developed to automate the previously manual task of assigning concrete pour times to sensor data, a critical aspect for the strength prediction model. Additionally, the transition to Azure SQL Server from SQL Server Express marked a considerable upgrade in managing the vast amounts of data generated by our IoT devices. This enterprise-level solution was specifically optimized for IoT applications, enhancing efficiency, and enabling real-time data analysis and decision-making.

Another significant advancement was the implementation of Firmware Over the Air (FOTA) for datalogger firmware updates. During previous studies, updates were manually loaded onto each device using a USB programmer, a method unfeasible for updating thousands of devices nationwide. Using FOTA, we can deliver updates wirelessly over LTE, programming the devices automatically. This process necessitated two major components—the development of hardware and firmware capable of supporting wireless updates, and the establishment of a cloud system for managing and deploying these updates. The migration to Azure played a crucial role in this, creating the infrastructure necessary for effective FOTA management. Our firmware team's updates are now automatically transmitted to the cloud, with notifications sent for initiating wireless updates on a device-to-device basis, ensuring minimal disruption to the end user.

4. FIELD IMPLEMENTATION

This chapter contains the field implementations of the proposed sensor and sensing system. Our engineer team traveled across eight States during the period of this research and implemented our sensing system to real-world projects. Table 4.1 summarizes all field testing we have done since the invention of this technology. Figure 4.1 shows the States we have visited and Figure 4.2 shows our engineers in the field implementation.

TABLE 4.1
Field Testing Summary Table

	State	Date	Location	Structure
1	California	09/15/2023	Sacramento	H-50 Pavement
2	North Dakota	08/31/2023	Beach	I-94 Pavement
3	North Dakota	08/28/2023	Fargo	I-94 Pavement
4	Texas	08/16/2023	Arlington	I-30 Pavement
5	Texas	08/14/2023	Lubbock	FM1585 Pavement
6	Colorado	08/11/2023	Denver	Airport Pavement
7	Colorado	08/08/2023	Spring	Pavement
8	Kansas	08/03/2023	Leoti	KS-96 Pavement
9	Kansas	08/01/2023	Topeka	I-70 Patch
10	Indiana	07/25/2023	Indianapolis	I-69 Pavement
11	Missouri	07/17/2023	Rolla	I-44 Pavement
12	Tennessee	07/13/2023	Jackson	I-40 Pavement
13	Tennessee	07/12/2023	Jackson	I-40 Wall
14	Texas	08/29/2022	Hillsboro	I-35 Pavement
15	Indiana	07/11/2022	Lapel	Individual Slab
16	Indiana	09/02/2022	Fort Wayne	Bass Rd Pavement
17	Indiana	11/15/2020	West Lafayette	Building Slab
18	Indiana	10/12/2020	Fort Wayne	I-469 Bridge Deck
19	Indiana	07/20/2019	Indianapolis	I-465 Patch
20	Indiana	07/01/2019	Plainfield	I-70 Patch
21	Indiana	06/11/2019	Batesville	I-74 Pavement

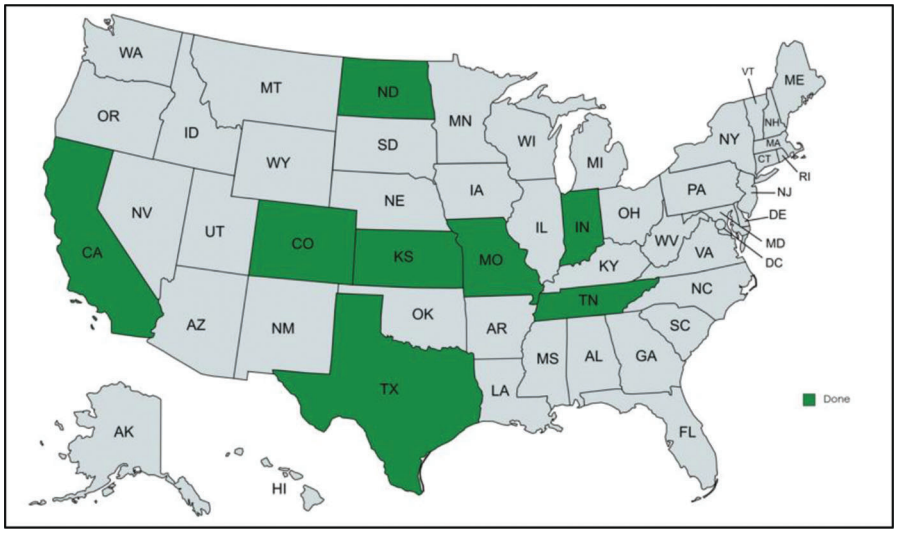

Figure 4.1 The US map of states where we implemented the sensing system.

4.1 Indiana I-69 Patching Project

On July 25, 2023, a pavement patching project was undertaken along the I-69 highway. The thickness of the pavement is 11 inches with continuous reinforcements (Figure 4.3 and Figure 4.4). Rui He, a PhD student at Purdue University, was on-site to install REBEL sensors along with dataloggers. The INDOT engineering team prepared one standard concrete beam sample, 6 inches by 6 inches by 22 inches, in order to assess the strength development of concrete under various curing conditions. In total, six (6) sensors were used in this project, including three (3) in the pavement, and three (3) in the beam cured on site, as shown in Figure 4.5. The reason for beam samples preparation is that we believe beam may have similar strength development profile and thermal profile as cylinders because the size and volume are closer to that of cylinder.

We compared the sensing results of the pavement and the beam sample with the compression results of 4″ by 8″ cylinders those were prepared and cured in the field, alongside the pavement structure. Two core samples were drilled from the pavement on the 7th day for the evaluation of the in-place reference strength. The primary metric to quantify the relative error of

Figure 4.2 Our engineer team on site.

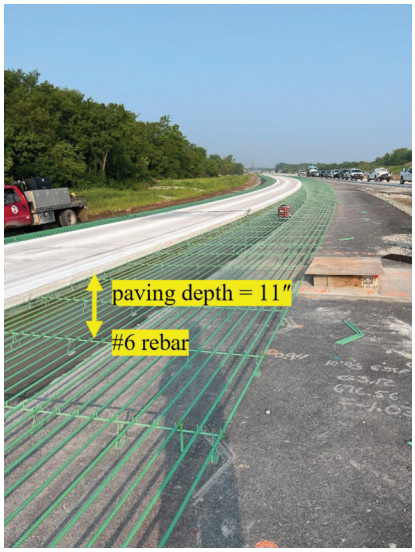

Figure 4.3 Reinforcements for the pavement.

sensing results regarding the cylinder results is mean absolute percentage error (MAPE), which takes the average of relative percentage error over various concrete ages, such as 1, 3, and 7 days. Our observations are as follows.

1. The MAPE of the sensing result is 24.5% and 18.3% higher than the cylinder test results, respectively for the pavement and beam sample, as shown in Figure 4.6 and Figure 4.7.
2. Core drill sample strength is close to the cylinder sample, while the corresponding sensing results of the pavement are higher than the strength of core drill sample.
3. This can be attributed to the damage to the core samples during core drilling process. According to the study performed by Alabama DOT and ACI318-14 26.12. 4.1(d), it is recommended that an average of core strength of 85% or greater of the design strength can be deemed as structurally adequate.
4. In addition, the design strength is a conservative estimation of actual strength with 95% confidence level, so the actual strength is expected to be more than 15% higher than the core sample results.
5. Therefore, we believe that our sensing results are more accurate than core drill results and closer to the actual in place strength of concrete.

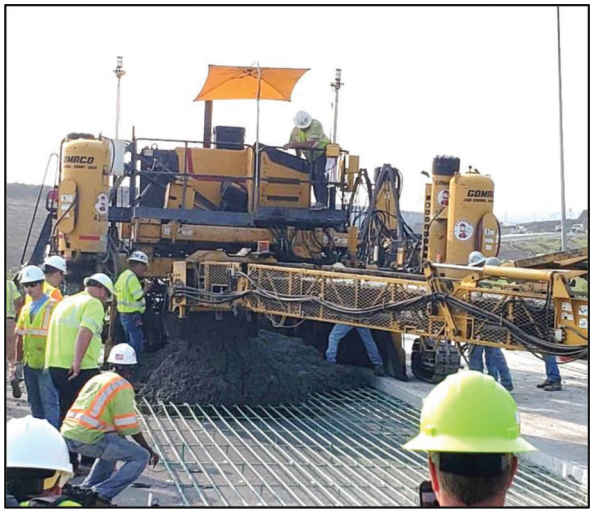

Figure 4.4 The placement of concrete through a paver.

We have observed that the sensor reading in pavement (24.5%) is higher than that of beam (18.3%) by 6.2%. This can be justified by examining the temperature profiles presented in Figure 4.8.

The temperature data of concrete pavement versus that of the beam agrees with our sensing results, therefore validating our hypothesis the strength development in pavement is higher than the beam sample due to the different in thermal mass and the speed of moisture lost.

Figure 4.8 also indicates the similarity between the temperature profiles of the pavement and the beam at early age (first 24 hours), which agrees with the higher sensing results of the beam sample than compression results of cylinders.

In conclusion, our initial dataset has effectively shown the potential of the REBEL sensor in accurately measuring the in-place strength of concrete structures. The sensor results obtained from both the concrete beam and pavement tests align more closely with the actual in-place strengths than the outcomes of cylinder breaking tests. However, we did notice some variance in the readings from the three sensors, approximately 20%. This discrepancy is largely attributed to the fact that currently, all sensors are manually crafted in Professor Lu's research laboratory at Purdue University. We are confident that adopting a standardized manufacturing process will significantly reduce these variations.

Figure 4.5 Beam and cylinder samples prepared on site.

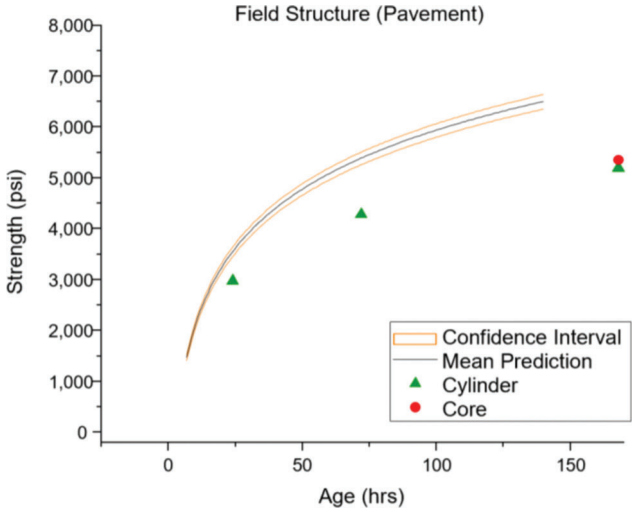

Figure 4.6 The sensing results of I-69 pavement.

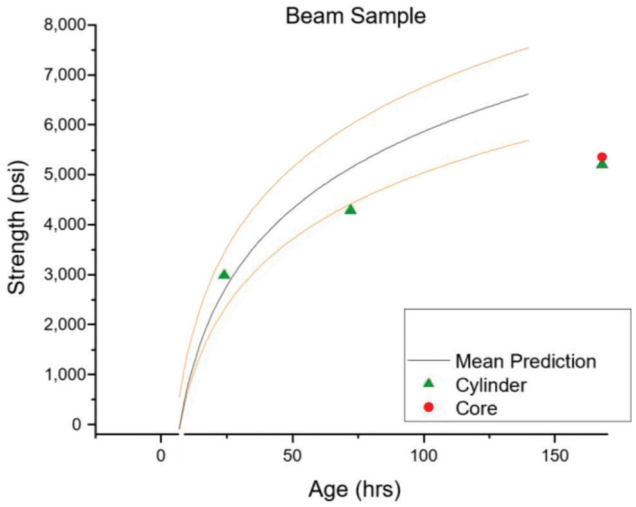

Figure 4.7 The sensing results of I-69 beam sample.

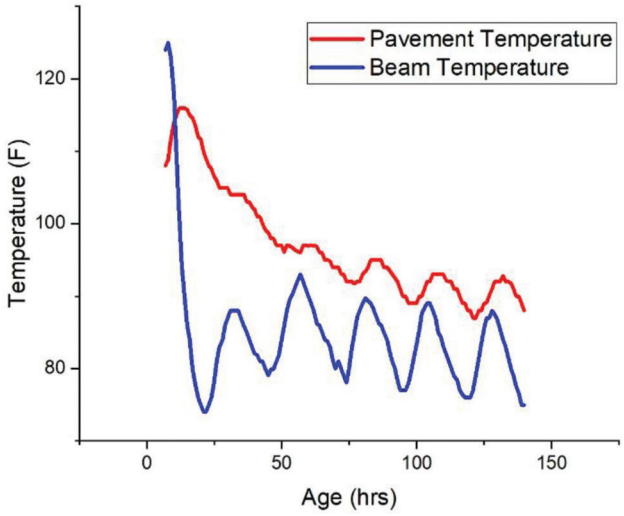

Figure 4.8 The temperature data of I-69 pavement and beam sample.

We have observed that the sensor reading in pavement is higher than that of beam and cylinder testing by 8% on average, as shown in Figure 4.6 and Figure 4.7.

The variance in sensing results among the beam and pavement can be rationalized by examining the temperature profiles presented in Figure 4.8. The temperature data of concrete pavement versus lab cured beam agrees with our sensing results, therefore validating our hypothesis the strength development in pavement is higher than the 4 by 8 inches of cylinder due to large different in thermal mass and the speed of moisture lost.

4.2 Kansas I-70 Patching and KS-96 Paving Project

4.2.1 I-70 Patching Project

On August 1, 2023, a pavement patching project was undertaken along the I-70 highway. The thickness of the pavement is 6 inches. Rui He, a PhD student at Purdue University, was on-site to install REBEL sensors along with dataloggers. The KDOT engineering team prepared one standard concrete beam sample, 6 inches by 6 inches by 22 inches, in order to assess the strength development of concrete under various curing conditions. In total, six (6) sensors were used in this project, including three (3) in the pavement, and three (3) in the beam cured under laboratory conditions. The reason for beam preparation is that we believe beam may have similar strength development profile and thermal profile because the size and volume are closer to that of cylinder.

4.2.2 KS-96 Paving Project

On August 3, 2023, a pavement patching project was undertaken along the KS-96 highway. The thickness of the pavement is 9 inches. Rui He was on-site to install REBEL sensors along with dataloggers. The KDOT engineering team prepared one standard concrete beam sample, 6 inches by 6 inches by 22 inches, in order to assess the strength development of concrete under various curing conditions. In total, six (6) sensors were used in this project, including three (3) in the pavement, and three (3) in the beam cured under laboratory conditions.

4.2.3 Sensing Results of Concrete Strength

The sensing results and cylinder break results are presented in Figure 4.9 and Figure 4.11, respectively for I-70 and KS-96 project. Each prediction curve represents the mean value of three (3) sensors. The team has observed discrepancies among sensor outputs, primarily attributed to the inconsistent quality of sensors and dataloggers, as they are handmade in Lu's lab at Purdue University. Consequently, the post processed mean value of the sensing results in each beam (or pavement) was used as the result, a process similar to that outlined in ASTM C39 Section 11.1.

4.2.4 Discussion

We have observed that for both I-70 patching and KS-96 paving jobs, the sensor reading in pavement is higher than that of beam and cylinder testing by 15% on average.

The variance in sensing results among the beam and pavement can be rationalized by examining the temperature profiles presented in Figure 4.10 and Figure 4.12. The temperature data of concrete pavement versus lab cured beam agrees with our sensing results, therefore validating our hypothesis the strength development in pavement is higher than the 4 by 8 inches of cylinder due to large different in thermal mass and the speed of moisture lost.

We noticed that for I-70 patching job, the sensing result for the concrete beam is higher than that of

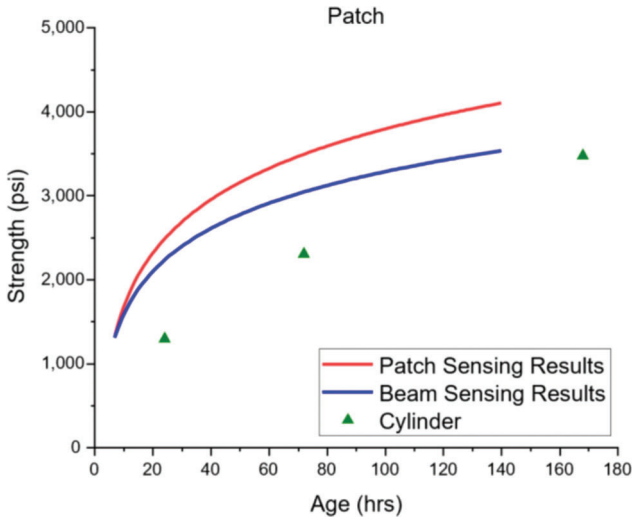

Figure 4.9 The sensing results of I-70 pavement and beam sample.

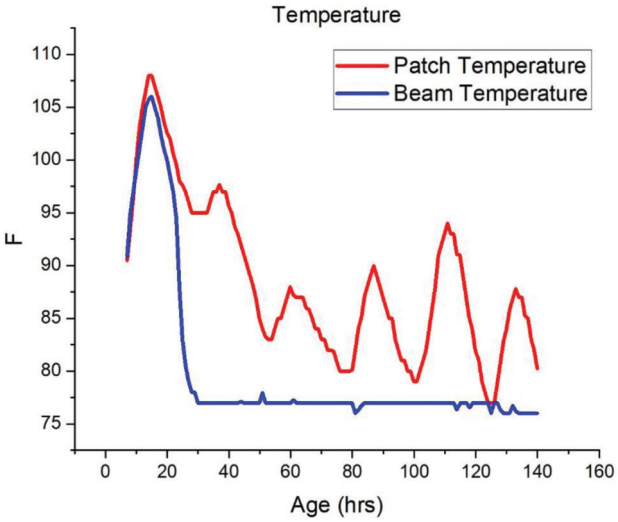

Figure 4.10 The temperature data of I-70 pavement and beam sample.

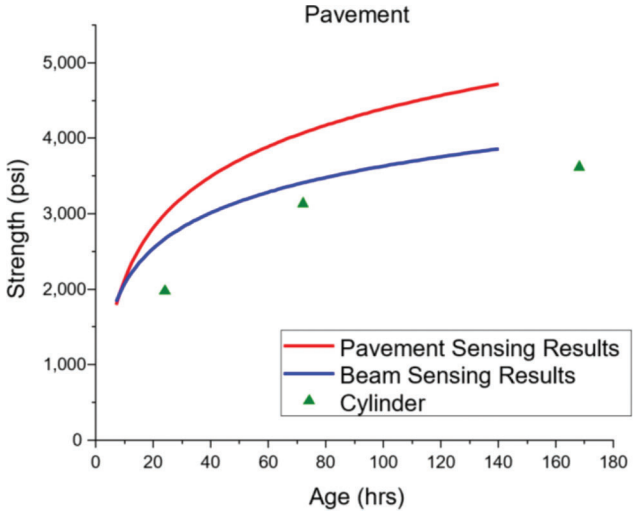

Figure 4.11 The sensing results of KS-96 pavement and beam sample.

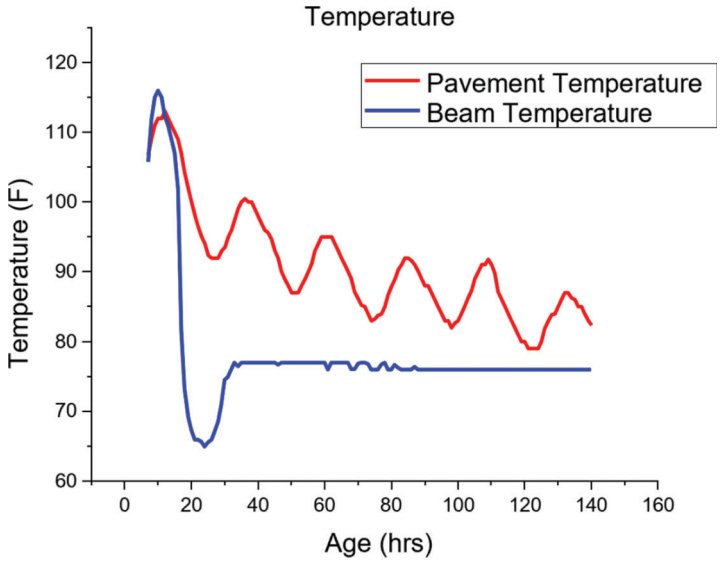

Figure 4.12 The temperature data of KS-96 pavement and beam sample.

cylinder break. However, for KS-96 paving project, the sensing result for the concrete beam aligns closely with cylinder results as shown in Figure 4.11.

The reason for this can be explained by the concrete mixtures used in the two projects. For I-70 patching job, (1) this mixture contains plastic fibers (see Figure 4.13), which may cause the inhomogeneity of the concrete mix, and (2) the aggregates have three phases, i.e., fine, intermedium, and coarse which is different from that KS-96 job.

The mean values of three sensors resulting in concrete beams are comparable to those obtained through cylinder testing and maturity testing within the same concrete structure.

Figure 4.13 The fresh concrete with polymer fibers for KS-96 project.

4.3 North Dakota I-94 Paving Projects

4.3.1 I-94 Paving Job at Fargo, ND

On August 28, 2023, a paving project was undertaken along the I-94 highway at Fargo, ND. The thickness of the pavement is 10 inches. Rui He, a PhD student at Purdue University, was on-site to install REBEL sensors along with dataloggers. The NDDOT engineering team prepared one standard concrete beam sample, 6 inches by 6 inches by 22 inches, in order to assess the strength development of concrete under various curing conditions. In total, six (6) sensors were used in this project, including three (3) in the pavement, and three (3) in the beam cured under laboratory conditions. The reason for beam preparation is that we believe beam may have similar strength development profile and thermal profile because the size and volume are closer to that of cylinder.

4.3.2 I-94 Paving Job at Beach, ND

On August 31, 2023, a paving project was undertaken along the I-94 highway at Beach, ND. The thickness of the pavement is 9 inches. Rui He was on-site to install REBEL sensors along with dataloggers. The NDDOT engineering team prepared one standard concrete beam sample, 6 inches by 6 inches by 22 inches, in order to assess the strength development of concrete under various curing conditions. In total, six (6) sensors were used in this project, including three (3) in the pavement, and three (3) in the beam cured under laboratory conditions.

4.3.3 Sensing Results of Concrete Strength

The sensing results and cylinder break results are presented in Figure 4.14 and Figure 4.16, respectively for I-94 at Fargo and I-94 at Beach project. The post

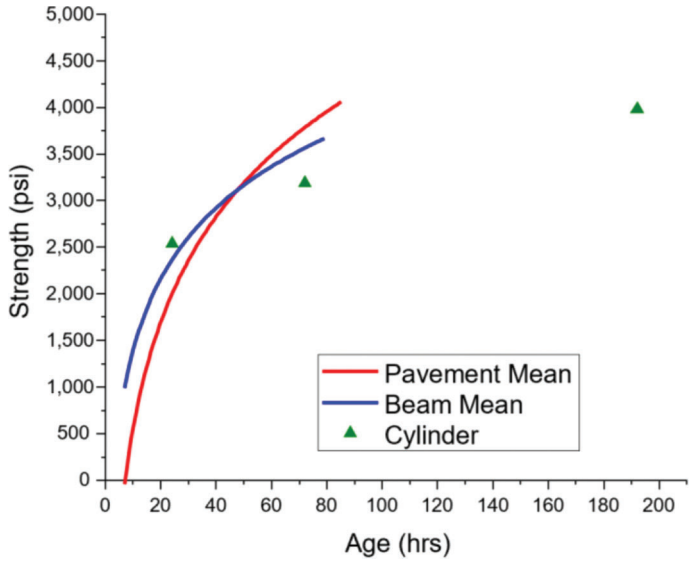

Figure 4.14 The sensing results of I-94 (Fargo, ND) pavement and beam sample.

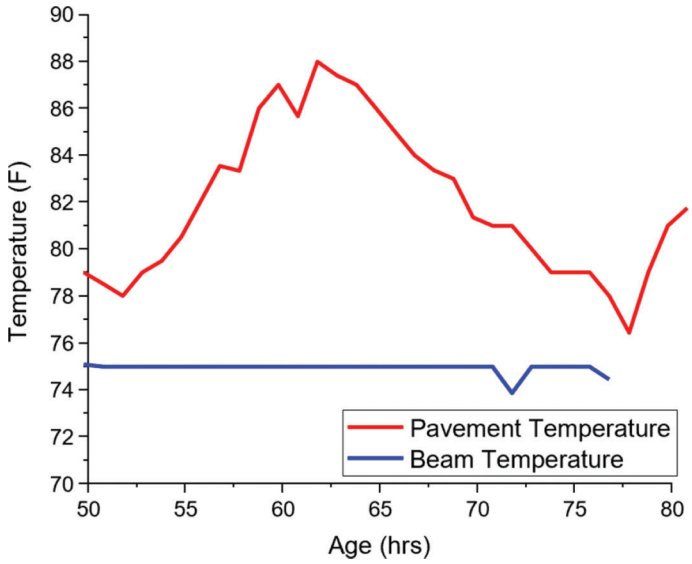

Figure 4.15 The temperature data of I-94 (Fargo, ND) pavement and beam sample.

processed mean value of the sensing results in each beam (or pavement) was used as the result, a process similar to that outlined in ASTM C39 Section 11.1.

4.3.4 Discussion

We have observed that for both paving jobs, the sensor reading in pavement is higher than that of beam and cylinder testing by 5% on average.

The variance in sensing results among the beam and pavement can be rationalized by examining the temperature profiles presented in Figure 4.15 and Figure 4.17. The temperature data of concrete pavement versus lab cured beam agrees with our sensing results, therefore validating our hypothesis the strength development in pavement is higher than the 4 by 8 inches of cylinder due to large different in thermal mass and the speed of moisture lost.

We observed the data length is short (total length is less than 80 hours, and temperature data not available preceding the 50th hour) for the Fargo sensing results. This is due to the failure of the LTE module (the wireless transmission module) of our data loggers. We will improve the quality of hardware through a standard manufacturing process.

The mean values of sensing results of three sensors in concrete beams are comparable to those obtained through cylinder testing and maturity testing within the same concrete structure.

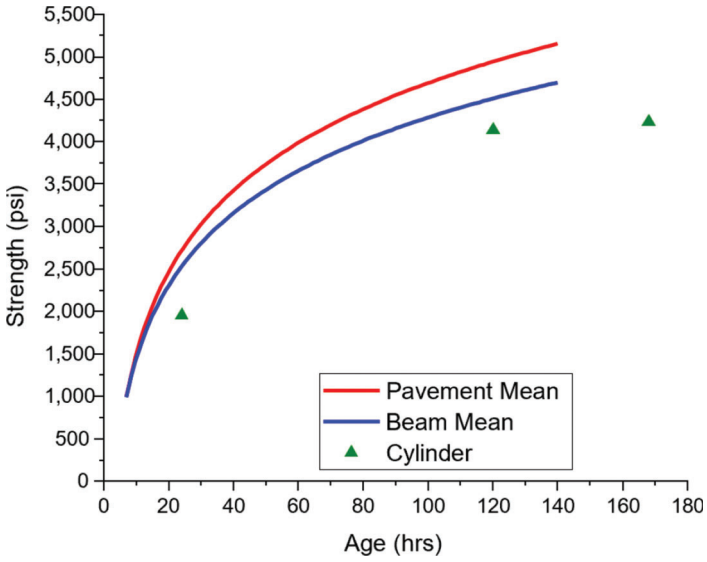

Figure 4.16 The sensing results of I-94 (Beach, ND) pavement and beam sample.

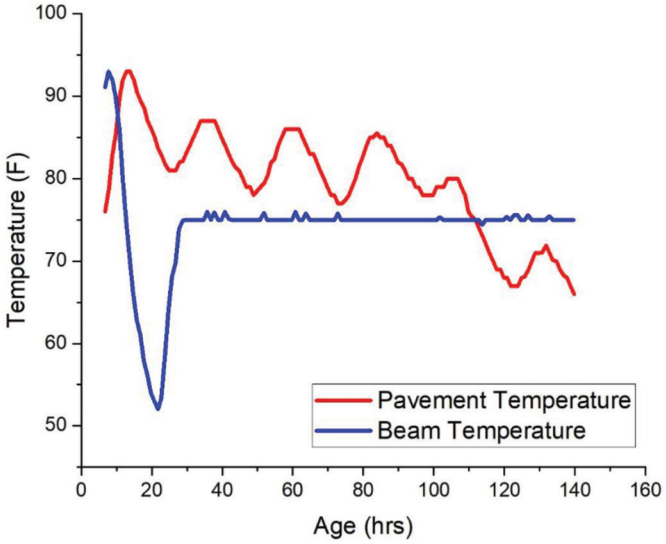

Figure 4.17 The temperature data of I-94 (Beach, ND) pavement and beam sample.

4.4 California H-50 Paving Project

On September 15, 2023, a construction project was undertaken along the Highway-50 Corridor. The pavement for this project consisted of a continuously reinforced concrete slab. Rui He, a PhD student at Purdue University, was on-site to install REBEL sensors along with dataloggers. The Caltrans engineering team prepared two standard concrete beam samples, each measuring 6 inches by 6 inches by 22 inches, to assess the strength development of concrete under various curing conditions. In total, nine (9) sensors were embedded, including three (3) in the pavement, three (3) in the on-site cured beam, and three (3) in the beam cured under laboratory conditions.

4.4.1 Sensing Results of Concrete Strength

The sensing results and cylinder break results are presented in the Figure 4.18. Each prediction curve represents the mean value of three (3) sensors, which were generated using a proprietary machine learning (ML) algorithm to convert sensor output along with temperature profile into compressive strength. The team has observed discrepancies among sensor outputs, attributed to the inconsistent quality of the hand-made sensors and dataloggers at Lu's lab as well as intrinsic material inhomogeneity of concrete. Consequently, the post processed mean value of the sensing results in each beam (or pavement) was used as the result, a process similar to that outlined in ASTM C39 Section 11.1.

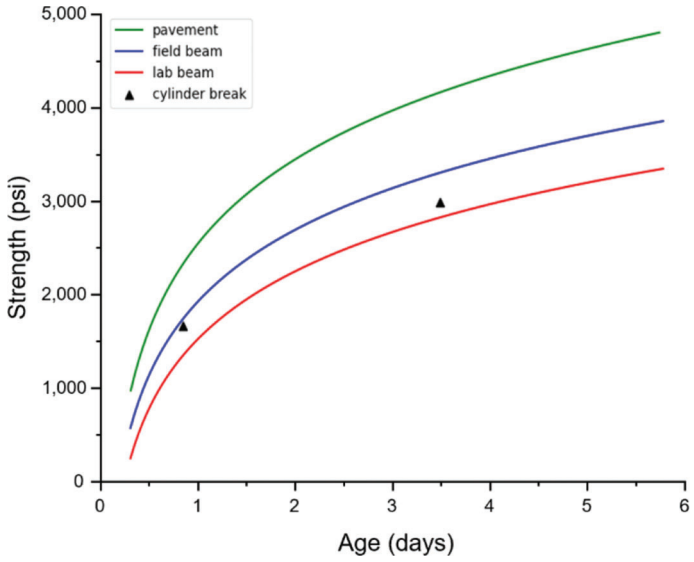

Figure 4.18 The sensing results of H-50 pavement and beam samples.

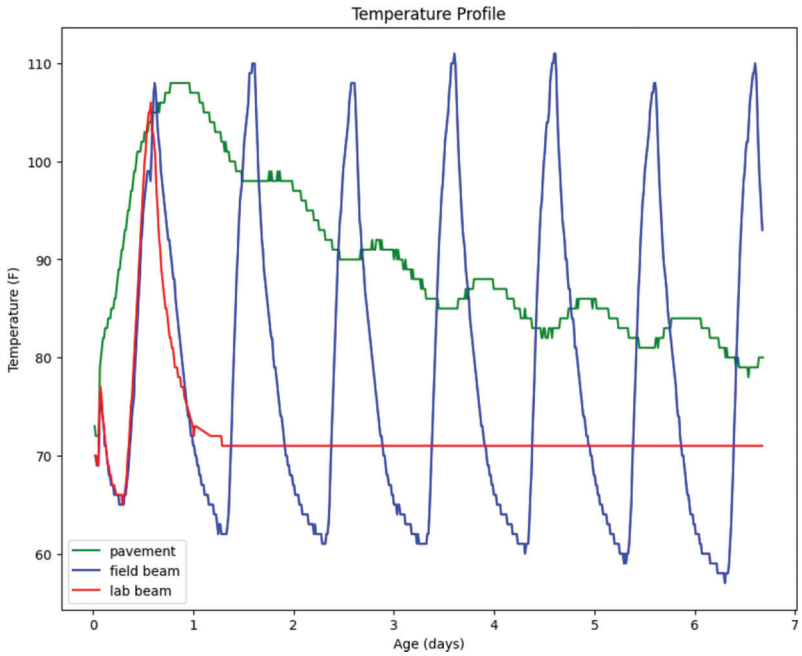

Figure 4.19 The temperature data of H-50 pavement and beam samples.

As shown in Figure 4.18, the sensing results for two concrete beams (one cured on site and the other in the lab) closely align with that of cylinder break as per ASTM C39. However, the results of sensors embedded in the pavement are substantially higher, as explained below.

The variance in sensing results among the beam and pavement can be rationalized by examining the temperature and maturity profiles presented in the Figure 4.19 and Figure 4.20. The maturity data of three concrete structures (lab cured beam, field cured beam and pavement) agrees with our sensing results, therefore validating our hypothesis that difference in strength between the pavement and cylinder was caused by the significant difference of thermal profile for pavement and beam.

The mean values of sensing results are comparable to those obtained through cylinder testing and maturity testing within the same concrete structure. As explained earlier, all sensors and dataloggers were handcrafted in our research lab at this stage, leading to significant discrepancies among the three sensors. This issue can be addressed by implementing a standard manufacturing process. We are currently collaborating with manufacturing partners to ensure the quality and consistency of both the sensors and dataloggers.

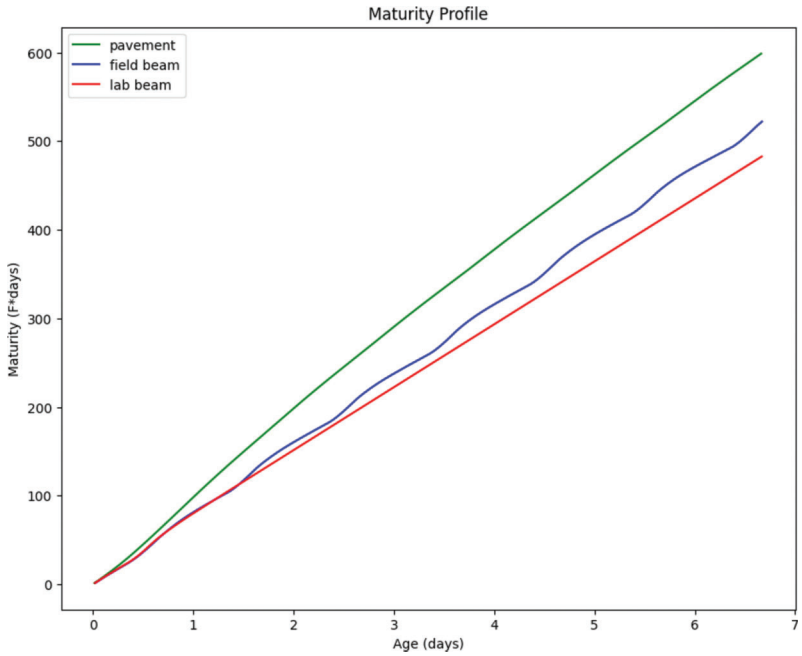

Figure 4.20 The maturity data of H-50 pavement and beam samples.

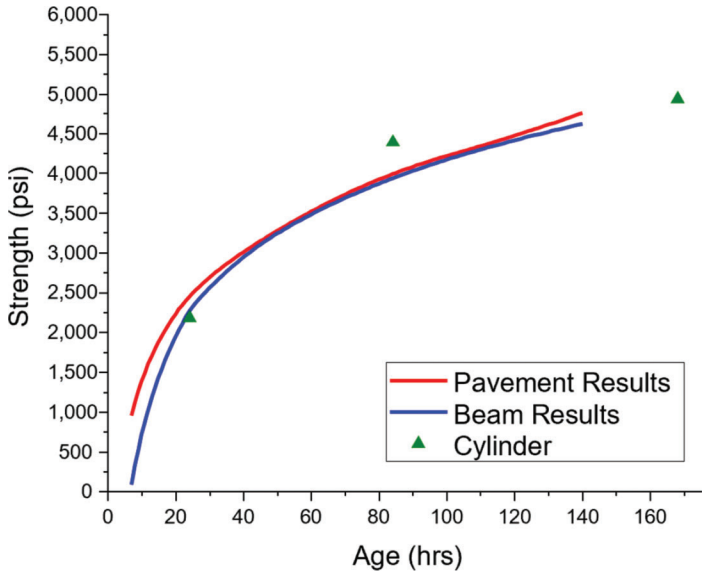

Figure 4.21 The sensing results of I-44 pavement and beam samples.

4.5 Missouri I-44 Paving Project

On July 17, 2023, a construction project was undertaken along the I-44 highway. The pavement for this project consisted of a PCCP concrete slab. Rui He, a PhD student at Purdue University, was on-site to install REBEL sensors along with dataloggers. The MDOT engineering team prepared a standard concrete beam sample, each measuring 6 inches by 6 inches by 22 inches, to assess the strength development of concrete under various curing conditions. In total, six (6) sensors were embedded, including three (3) in the pavement and three (3) in the on-site cured beam.

4.5.1 Sensing Results of Concrete Strength

The sensing results and cylinder break results are presented in the Figure 4.21. Each prediction curve represents the mean value of three (3) sensors, which were generated using a proprietary machine learning (ML) algorithm to convert sensor output along with temperature profile into compressive strength. The team has observed discrepancies among sensor outputs, attributed to the inconsistent quality of the hand-made sensors and dataloggers at Lu's lab as well as intrinsic material inhomogeneity of concrete. Consequently, the post processed mean value of the sensing results in each

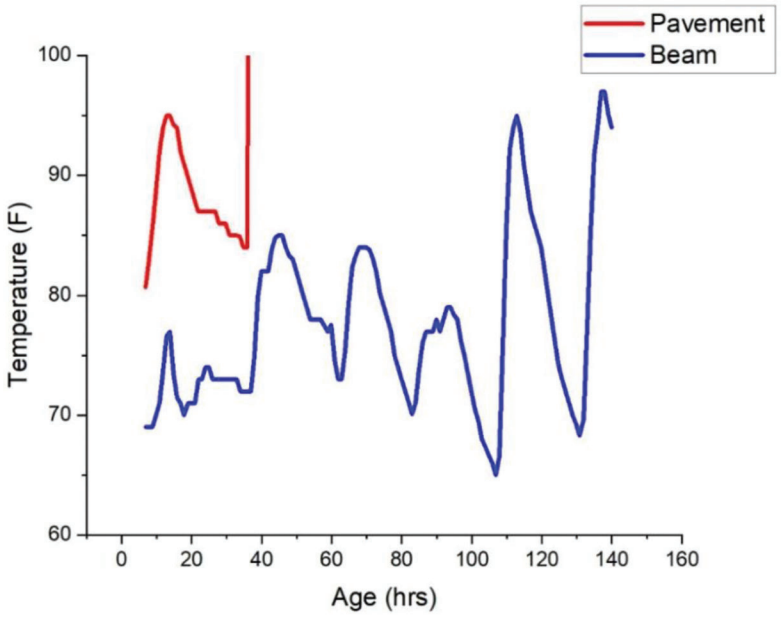

Figure 4.22 The temperature data of I-44 pavement and beam samples.

beam (or pavement) was used as the result, a process similar to that outlined in ASTM C39 Section 11.1.

As shown in Figure 4.21, the sensing results for the concrete and the pavement closely align with that of cylinder break as per ASTM C39. The result for the pavement is slightly higher than that of the beam.

The temperature data in Figure 4.22 agrees with our sensing results, therefore validating our hypothesis that difference in strength between the pavement and cylinder was caused by the difference of thermal profile for pavement and beam.

4.6 Texas FM-1585 and I-30 Paving Project

4.6.1 FM-1585 Paving Project

On August 14, 2023, a construction project was undertaken along the FM-1585 highway. The pavement for this project consisted of a continuously reinforced concrete slab. Rui He, a PhD student at Purdue University, was on-site to install REBEL sensors along with dataloggers. The TXDOT engineering team prepared a standard concrete beam sample, each measuring 6 inches by 6 inches by 22 inches, to assess the strength development of concrete under various curing conditions. In total, six (6) sensors were embedded, including three (3) in the pavement, and three (3) in the on-site cured beam.

4.6.2 Sensing Results of Concrete Strength

The sensing results and cylinder break results are presented in the Figure 4.23. Each prediction curve represents the mean value of three (3) sensors, which were generated using a proprietary machine learning (ML) algorithm to convert sensor output along with temperature profile into compressive strength. The team has observed discrepancies among sensor outputs, attributed to the inconsistent quality of the hand-made sensors and dataloggers at Lu's lab as well as intrinsic material inhomogeneity of concrete. Consequently, the post processed mean value of the sensing results in each beam (or pavement) was used as the result, a process similar to that outlined in ASTM C39 Section 11.1.

As shown in Figure 4.23, the sensing results for the concrete and the pavement closely align with that of cylinder break as per ASTM C39. The result for the pavement is slightly higher than that of the beam.

The temperature data in Figure 4.24 agrees with our sensing results, therefore validating our hypothesis that difference in strength between the pavement and cylinder was caused by the difference of thermal profile for pavement and beam.

4.6.3 I-30 Paving Project

On August 16, 2023, a construction project was undertaken along the I-30 highway. The pavement for this project consisted of a continuously reinforced concrete slab. Rui He, a PhD student at Purdue University, was on-site to install REBEL sensors along with dataloggers. The TXDOT engineering team prepared a standard concrete beam sample, each measuring 6 inches by 6 inches by 22 inches, to assess the strength development of concrete under various curing conditions. In total, six (6) sensors were embedded, including three (3) in the pavement and three (3) in the on-site cured beam.

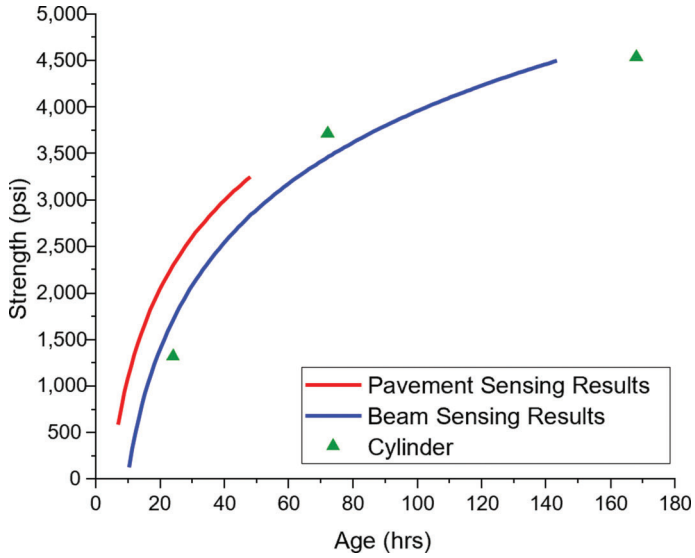

Figure 4.23 The sensing results of FM-1585 pavement and beam samples.

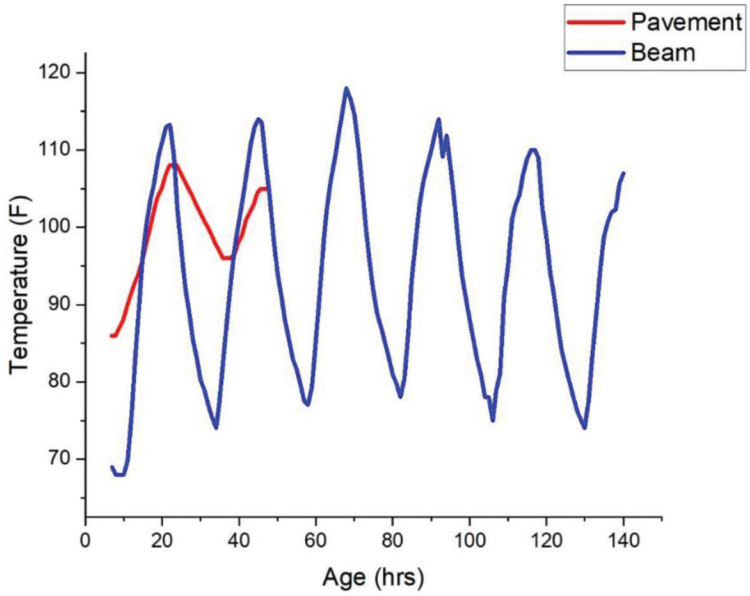

Figure 4.24 The temperature data of FM-1585 pavement and beam samples.

4.6.4 Sensing Results of Concrete Strength

The sensing results and cylinder break results are presented in the Figure 4.25. Each prediction curve represents the mean value of three (3) sensors, which were generated using a proprietary machine learning (ML) algorithm to convert sensor output along with temperature profile into compressive strength. The team has observed discrepancies among sensor outputs, attributed to the inconsistent quality of the hand-made sensors and dataloggers at Lu's lab as well as intrinsic material inhomogeneity of concrete. Consequently, the post processed mean value of the sensing results in each beam (or pavement) was used as the result, a process like that outlined in ASTM C39 Section 11.1.

As shown in Figure 4.25, the sensing results for the concrete and the pavement closely align with that of cylinder break as per ASTM C39. The result for the pavement is slightly higher than that of the beam.

The temperature data in Figure 4.26 agrees with our sensing results, therefore validating our hypothesis that difference in strength between the pavement and cylinder was caused by the difference of thermal profile for pavement and beam.

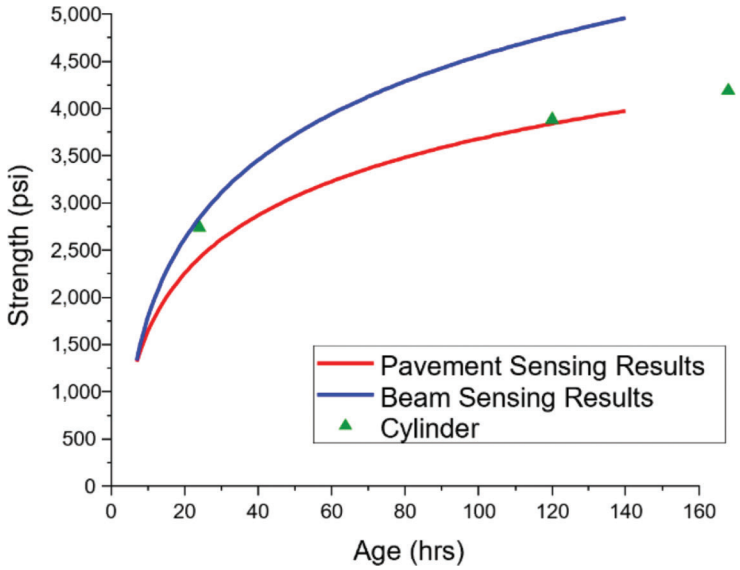

Figure 4.25 The sensing results of I-30 pavement and beam samples.

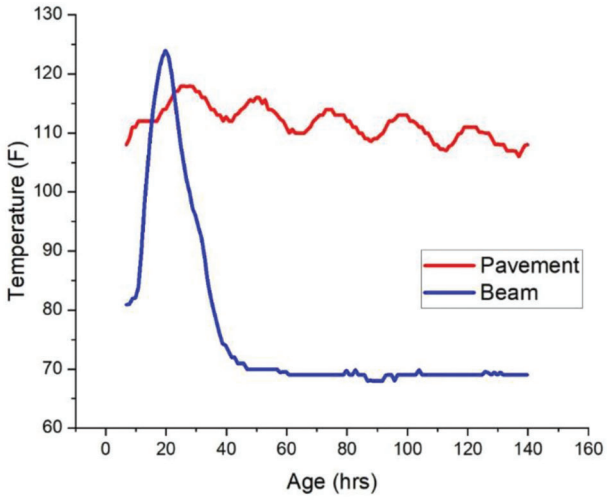

Figure 4.26 The temperature data of I-30 pavement and beam samples.

5. CONCLUSIONS

This project has marked a significant milestone in the development of embedded sensor and datalogger technologies. We have successfully enhanced the connectivity process, evidenced by the integration of QR code scanning, which has streamlined the deployment process and minimized errors. The establishment of a full-scale manufacturing process, encompassing a robust supply chain and strategic design modifications, has set a new standard in the production of our sensing systems.

A pivotal aspect of our project was the optimization of the IoT cloud infrastructure. The transition to Microsoft Azure from AWS EC2 represents a leap forward in terms of scalability, resilience, and the integration of microservices, ensuring that our technology remains at the forefront of innovation. The field implementation and testing across various states have been instrumental in demonstrating the practicality and robustness of our technology. These real-world applications not only validated our systems but also provided invaluable insights into their performance under diverse conditions.

In conclusion, this project has not only achieved its objectives but has also set a new benchmark in sensor and datalogger technology. We are confident for future growth and innovation, and our commitment to excellence will continue to drive our efforts in this ever-evolving field.

REFERENCES

ASTM. (2016). *ASTM C597-16: Standard test method for pulse velocity through concrete*. ASTM International. https://doi.org/10.1520/C0597-16

ASTM. (2017). *ASTM C1074-17: Practice for estimating concrete strength by the maturity method*. ASTM International.

ASTM. (2022). *ASTM C1383-15: Standard test method for measuring the P-wave speed and the thickness of concrete plates using the impact-echo method*. ASTM International.

Bogas, J. A., Gomes, M. G., & Gomes, A. (2013, July). Compressive strength evaluation of structural lightweight concrete by non-destructive ultrasonic pulse velocity method. *Ultrasonics*, *53*(5), 962–972. https://doi.org/10.1016/j.ultras.2012.12.012

Carino, N. J. (2001, May). The impact-echo method: An overview. *Structures 2001: A Structural Engineering Odyssey* (pp. 1–18). American Society of Civil Engineers. https://doi.org/10.1061/40558(2001)15

Carino, N. J. (2015, September 15–17). *Impact echo: The fundamentals* [Symposium]. International Symposium Non-Destructive Testing in Civil Engineering (NDT-CE). Berlin, Germany.

Casciaro, S., Pisani, P., Conversano, F., Renna, M. D., Soloperto, G., Casciaro, E., Quarta, E., Grimaldi, A., & Muratore, M. (2016, January). Innovative ultrasound approach to estimate spinal mineral density: diagnostic assessment on overweight and obese women. *IET Science, Measurement & Technology*, *10*(1), 1–9. https://doi.org/10.1049/iet-smt.2015.0056

del Viso, J. R., Carmona, J. R., & Ruiz, G. (2008, March). Shape and size effects on the compressive strength of high-strength concrete. *Cement and Concrete Research*, *38*(3), 386–395. https://doi.org/10.1016/j.cemconres.2007.09.020

Fan, S., Zhao, S., Qi, B., & Kong, Q. (2018, May). Damage evaluation of concrete column under impact load using a piezoelectric-based EMI technique. *Sensors*, *18*(5), 1591. https://doi.org/10.3390/s18051591

Ghafari, E., Yuan, Y., Wu, C., Nantung, T., & Lu, N. (2018, May). Evaluation the compressive strength of the cement paste blended with supplementary cementitious materials using a piezoelectric-based sensor. *Construction and Building Materials*, *171*, 504–510. https://doi.org/10.1016/j.conbuildmat.2018.03.165

Gibson, A., & Popovics, J. S. (2005, April). Lamb wave basis for impact-echo method analysis. *Journal of Engineering Mechanics*, *131*(4), 438–443. https://doi.org/10.1061/(ASCE)0733-9399(2005)131:4(438)

Han, G., Su, Y.-F., Nantung, T., & Lu, N. (2020, November). Mechanism for using piezoelectric sensor to monitor strength gain process of cementitious materials with the temperature effect. *Journal of Intelligent Material Systems and Structures*, *32*(10), 1128–1139. https://doi.org/10.1177/1045389X20974441

Irrigaray, M. A. P., Pinto, R. C. de A., & Padaratz, I. J. (2016, June). A new approach to estimate compressive strength of concrete by the UPV method. *Revista IBRACON de Estruturas e Materiais*, *9*(3), 395–402. https://doi.org/10.1590/S1983-41952016000300004

Ju, M., Park, K., & Oh, H. (2017, December). Estimation of compressive strength of high strength concrete using non-destructive technique and concrete core strength. *Applied Sciences*, *7*(12), 1249. https://doi.org/10.3390/app7121249

Kong, Z., & Lu, N. (2020, November). Improved method to determine Young's modulus for concrete cylinder using electromechanical spectrum: Principle and validation. *Journal of Aerospace Engineering*, *33*(6), 04020079. https://doi.org/10.1061/(ASCE)AS.1943-5525.0001196

Kong, Z., & Lu, N. (2023). *Determining optimal traffic opening time through concrete strength monitoring: Wireless sensing* (Joint Transportation Research Program Publication No. FHWA/IN/JTRP-2023/05). West Lafayette, IN: Purdue University. https://doi.org/10.5703/1288284317613

Latif Al-Mufti, R., & Fried, A. N. (2012, December). The early age non-destructive testing of concrete made with recycled concrete aggregate. *Construction and Building Materials*, *37*, 379–386. https://doi.org/10.1016/j.conbuildmat.2012.07.058

Liang, C., Sun, F. P., & Rogers, C. A. (1994, January). An impedance method for dynamic analysis of active material systems. *Journal of Vibration and Acoustics*, *116*(1), 120–128. https://doi.org/10.1115/1.2930387

Lu, X., Lim, Y. Y., & Soh, C. K. (2018, July). A novel electromechanical impedance–based model for strength development monitoring of cementitious materials. *Structural Health Monitoring*, *17*(4), 902–918. https://doi.org/10.1177/1475921717725028

Narayanan, A., Kocherla, A., & Subramaniam, K. V. L. (2017, December). Embedded PZT sensor for monitoring mechanical impedance of hydrating cementitious materials. *Journal of Nondestructive Evaluation*, *36*(64). https://doi.org/10.1007/s10921-017-0442-4

Narayanan, A., Kocherla, A., & Subramaniam, K. V. L. (2020). Damage detection in concrete using surface mounted PZT transducers. *Materials Today: Proceedings*, *28*(Part 2), 925–930. https://doi.org/10.1016/j.matpr.2019.12.326

Popovics, J. S. (1997, August). Effects of Poisson's Ratio on impact-echo test analysis. *Journal of Engineering Mechanics*, *123*(8), 843–851. https://doi.org/10.1061/(ASCE)0733-9399(1997)123:8(843)

Punurai, W., Jacobs, L. J., Kurtis, K. E., Jarzynski, J., & Qu, J. (2006, March). Characterization of entrained air voids using scattered ultrasound. *AIP Conference Proceedings*, *820*(1), 1335–1342. https://doi.org/10.1063/1.2184679

Punurai, W., Jarzynski, J., Qu, J., Kurtis, K. E., & Jacobs, L. J. (2006, September). Characterization of entrained air voids in cement paste with scattered ultrasound. *NDT & E International*, *39*(6), 514–524. https://doi.org/10.1016/j.ndteint.2006.02.001

Saravanan, T. J., Balamonica, K., Priya, C. B., Reddy, A. L., & Gopalakrishnan, N. (2015). Comparative performance of various smart aggregates during strength gain and damage states of concrete. *Smart Materials and Structures*, *24*(8), 085016.

Shariati, M., Ramli-Sulong, N. H., Shafigh, P., & Sinaei, H. (2011). Assessing the strength of reinforced concrete structures through ultrasonic pulse velocity and Schmidt rebound hammer tests. *Scientific Research and Essays*, *6*, 213–220.

Shin, S. W., Qureshi, A. R., Lee, J.-Y., & Yun, C. B. (2008, October). Piezoelectric sensor based nondestructive active monitoring of strength gain in concrete. *Smart Material Structures*, *17*(5), 055002. https://doi.org/10.1088/0964-1726/17/5/055002

Smith, K. (2005, November). *Maturity testing for concrete pavement applications tech brief* (Report No. FHWA-IF-06-004). Federal Highway Administration.

Su, Y.-F., Han, G., Amran, A., Nantung, T., & Lu, N. (2019, November). Instantaneous monitoring the early age properties of cementitious materials using PZT-based electro-mechanical impedance (EMI) technique. *Construction and Building Materials*, *225*, 340–347. https://doi.org/10.1016/j.conbuildmat.2019.07.164

Su, Y.-F., Han, G., Huang, C., Nantung, T., & Lu, N. (2021). Trial field implementation of piezoelectric sensing technique for in-place concrete evaluation. *ACI Materials Journal*, *118*(1), 147–156. https://doi.org/10.14359/51726998

Su, Y.-F., Han, G., Kong, Z., Nantung, T., & Lu, N. (2020). Embeddable piezoelectric sensors for strength gain monitoring of cementitious materials: The influence of coating materials. *Engineered Science*, *11*, 66–75. https://doi.org/10.30919/es8d1114

Su, Y.-F., Han, G., & Lu, N. (2020). *Determining the optimal traffic opening timing through an in-situ NDT method for concrete early age properties* (Joint Transportation Research Program Publication No. FHWA/IN/JTRP-2020/02). West Lafayette, IN: Purdue University. https://doi.org/10.5703/1288284317113

Su, Y.-F., Han, G., Nantung, T., & Lu, N. (2020, October). Novel methodology on direct extraction of the strength information from cementitious materials using piezo-sensor based electromechanical impedance (EMI) method. *Construction and Building Materials*, *259*, 119848. https://doi.org/10.1016/j.conbuildmat.2020.119848

Villain, G., Abraham, O., Marrec, L. L., & Rakotomanana, L. (2009, June 30–July 3). *Determination of the bulk elastic moduli of various concrete by resonance frequency analysis of slabs submitted to degradations* [Symposium]. NDTCE'09, Non-Destructive Testing in Civil Engineering Nantes, France.

Wang, D., Song, H., & Zhu, H. (2014, October). Embedded 3D electromechanical impedance model for strength monitoring of concrete using a PZT transducer. *Smart Materials and Structures*, *23*(11), 115019. https://doi.org/10.1088/0964-1726/23/11/115019

Yang, Y., & Divsholi, B. S. (2010, December). Sub-frequency interval approach in electromechanical impedance technique for concrete structure health monitoring. *Sensors*, *10*(12), 11644–11661. https://doi.org/10.3390/s101211644

Ye, G., Breugel, K. van, & Fraaij, A. L. A. (2003, February). Experimental study and numerical simulation on the formation of microstructure in cementitious materials at early age. *Cement and Concrete Research*, *33*(2), 233–239. https://doi.org/10.1016/S0008-8846(02)00891-8

About the Joint Transportation Research Program (JTRP)

On March 11, 1937, the Indiana Legislature passed an act which authorized the Indiana State Highway Commission to cooperate with and assist Purdue University in developing the best methods of improving and maintaining the highways of the state and the respective counties thereof. That collaborative effort was called the Joint Highway Research Project (JHRP). In 1997 the collaborative venture was renamed as the Joint Transportation Research Program (JTRP) to reflect the state and national efforts to integrate the management and operation of various transportation modes.

The first studies of JHRP were concerned with Test Road No. 1—evaluation of the weathering characteristics of stabilized materials. After World War II, the JHRP program grew substantially and was regularly producing technical reports. Over 1,600 technical reports are now available, published as part of the JHRP and subsequently JTRP collaborative venture between Purdue University and what is now the Indiana Department of Transportation.

Free online access to all reports is provided through a unique collaboration between JTRP and Purdue Libraries. These are available at http://docs.lib.purdue.edu/jtrp.

Further information about JTRP and its current research program is available at http://www.purdue.edu/jtrp.

About This Report

An open access version of this publication is available online. See the URL in the citation below.

Kong, Z., & Lu, N., (2024). *Field implementation of concrete strength sensor to determine optimal traffic opening time* (Joint Transportation Research Program Publication No. FHWA/IN/JTRP-2024/05). West Lafayette, IN: Purdue University. https://doi.org/10.5703/1288284317724